AEM
Journals.ASM.org

The Gene Cluster for *para*-Nitrophenol Catabolism Is Responsible for 2-Chloro-4-Nitrophenol Degradation in *Burkholderia* sp. Strain SJ98

Jun Min,[a,b] Jun-Jie Zhang,[a] Ning-Yi Zhou[a]

Key Laboratory of Agricultural and Environmental Microbiology, Wuhan Institute of Virology, Chinese Academy of Sciences, Wuhan, China[a]; University of Chinese Academy of Sciences, Beijing, China[b]

***Burkholderia* sp. strain SJ98 (DSM 23195) utilizes 2-chloro-4-nitrophenol (2C4NP) or *para*-nitrophenol (PNP) as a sole source of carbon and energy. Here, by genetic and biochemical analyses, a 2C4NP catabolic pathway different from those of all other 2C4NP utilizers was identified with chloro-1,4-benzoquinone (CBQ) as an intermediate. Reverse transcription-PCR analysis showed that all of the *pnp* genes in the *pnpABA1CDEF* cluster were located in a single operon, which is significantly different from the genetic organization of all other previously reported PNP degradation gene clusters, in which the structural genes were located in three different operons. All of the Pnp proteins were purified to homogeneity as His-tagged proteins. PnpA, a PNP 4-monooxygenase, was found to be able to catalyze the monooxygenation of 2C4NP to CBQ. PnpB, a 1,4-benzoquinone reductase, has the ability to catalyze the reduction of CBQ to chlorohydroquinone. Moreover, PnpB is also able to enhance PnpA activity *in vitro* in the conversion of 2C4NP to CBQ. Genetic analyses indicated that *pnpA* plays an essential role in the degradation of both 2C4NP and PNP by gene knockout and complementation. In addition to being responsible for the lower pathway of PNP catabolism, PnpCD, PnpE, and PnpF were also found to be likely involved in that of 2C4NP catabolism. These results indicated that the catabolism of 2C4NP and that of PNP share the same gene cluster in strain SJ98. These findings fill a gap in our understanding of the microbial degradation of 2C4NP at the molecular and biochemical levels.**

As a typical representative of the chloronitrophenols, 2-chloro-4-nitrophenol (2C4NP), with high toxicity to humans, is widely utilized in the chemical syntheses of the fungicide nitrofungin and the pesticide dicapthon (1, 2). Structurally, 2C4NP is a chemical analogue of *para*-nitrophenol (PNP) that was listed as a priority environmental pollutant by the U.S. Environmental Protection Agency. The microbial degradation of PNP has been extensively investigated, in which either the hydroquinone (HQ) pathway (3–6) or the hydroxyquinol (BT) pathway (7–11) has been elucidated at both the genetic and biochemical levels. In contrast, the study of the degradation of its chlorinated derivatives is limited, with no genetic or biochemical investigation reported. This is because they are more resistant to microbial degradation due to the simultaneous existence of chlorine and nitro groups.

To date, four pure bacterial cultures have been isolated on the basis of the ability to utilize 2C4NP as a sole carbon and energy source (1, 12–14), and three different pathways based on different intermediates present during its degradation have been proposed. *Rhodococcus imtechensis* RKJ 300 (14) and *Burkholderia* sp. strain RKJ 800 (12) were reported to degrade 2C4NP via the HQ pathway, whereas *Burkholderia* sp. strain SJ98 degraded 2C4NP with the formation of PNP, which was further degraded via the BT pathway (13, 15). On the other hand, *Arthrobacter* sp. strain SJCon was thought to degrade 2C4NP with chlorohydroquinone (CHQ) as the ring cleavage substrate (1). However, none of these pathways has been characterized at the genetic and biochemical levels.

In this study, a 2C4NP catabolic pathway in *Burkholderia* sp. strain SJ98 that is different from those of all other 2C4NP utilizers was characterized at the genetic and biochemical levels. To our surprise, chloro-1,4-benzoquinone (CBQ) and CHQ, rather than PNP, 4-nitrocatechol (4-NC), and BT, as previously proposed (13), were identified during 2C4NP degradation. On the other hand, the *pnpABA1CDEF* cluster in a signal operon was proved to be also responsible for 2C4NP degradation by this strain, in addition to PNP degradation. This study fills a gap in our understanding of the mechanism of microbial 2C4NP degradation.

MATERIALS AND METHODS

Bacterial strains, plasmids, primers, chemicals, media, and culture conditions. The bacterial strains and plasmids used in this study are described in Table 1, and the primers used are described in Table 2. *Burkholderia* strains and *Pseudomonas* sp. strain WBC-3 were grown at 30°C in minimal medium (MM) (16) with various carbon sources, and the ability to utilize a nitrophenol substrate (2C4NP or PNP) was determined by monitoring the growth of cells together with the consumption of the corresponding substrates. *Escherichia coli* strains were grown in lysogeny broth (LB) at 37°C. When necessary, 100 μg/ml of ampicillin, 50 μg/ml of kanamycin, 34 μg/ml of chloramphenicol, or 20 μg/ml of tetracycline was added to the medium. All reagents were purchased from Sigma Chemical Co. (St. Louis, MO, USA) or Fluka Chemical Co. (Buchs, Switzerland).

Biotransformation and intermediate identification. Biotransformation was performed as described previously (17), with minor modifications. Strains SJ98 and WBC-3 were grown with 2 mM glucose to an optical density at 600 nm (OD_{600}) of 0.3 and then induced with 0.3 mM 2C4NP or PNP for 5 h. Cells were harvested, washed twice, and diluted to an OD_{600} of 1.0 with phosphate buffer (20 mM, pH 7.4) and 1 mM 2,2′-dipyridyl. The cell suspension was incubated for 10 min before 2C4NP or PNP was added. Then 0.5-ml samples were withdrawn at regular intervals, mixed with an equal volume of methanol, and vortexed vigorously for 5

Received 26 June 2014 **Accepted** 25 July 2014
Published ahead of print 1 August 2014
Editor: R. E. Parales
Address correspondence to Ning-Yi Zhou, n.zhou@pentium.whiov.ac.cn.
Supplemental material for this article may be found at http://dx.doi.org/10.1128/AEM.02093-14.

doi:10.1128/AEM.02093-14

TABLE 1 Bacterial strains and plasmids used in this study

Strain or plasmid	Relevant genotype or characteristic(s)	Reference or source
Burkholderia sp. strains		
SJ98	PNP and 2C4NP utilizer, wild type	13
SJ98Δ*pnpA*	SJ98 mutant with *pnpA* gene deleted	This study
SJ98Δ*pnpA1*	SJ98 mutant with *pnpA1* gene deleted	This study
SJ98Δ*pnpA*(pRK415-*pnpA*)	*pnpA* gene complemented by pRK415-*pnpA* in SJ98Δ*pnpA*	This study
Pseudomonas sp. strain WBC-3	PNP degrader, wild type	6
E. coli strains		
DH5α	*supE44 lacU169* (φ80*lacZ*ΔM15) *recA1 endA1 hsdR17 thi-1 gyrA96 relA1*	Novagen
Rosetta(DE3)pLysS	F^- *ompT hsdS* (r_B^- m_B^+) *gal dcm lacY1*(DE3)/pLysSRARE (Cm^r)	Novagen
WM3064	Donor strain for conjugation, 2,6-diaminopimelic acid auxotroph, *thrB1004 pro thi rpsL hsdS lacZ*ΔM15 RP4-1360 Δ(*araBAD*)*567* Δ*dapA1341*::(*erm pir* [wild type])	30
Plasmids		
pET-28a	Expression vector, Kan^r	Novagen
pTn*Mod*-Okm	Source of kanamycin resistance gene	28
pEX18Tc	Gene knockout vector, $oriT^+$ $sacB^+$ Tc^r	29
pRK415	Broad host range vector, Tc^r	32
pET-*pnpA*	NdeI-XhoI fragment containing *pnpA* inserted into pET-28a	This study
pZWJJ009	NdeI-XhoI fragment containing *pnpA* from WBC-3 inserted into pET-28a	6
pET-*pnpA1*	NdeI-XhoI fragment containing *pnpA1* inserted into pET-28a	This study
pET-*pnpB*	NdeI-XhoI fragment containing *pnpB* inserted into pET-28a	This study
pET-*pnpCD*	NdeI-XhoI fragment containing *pnpCD* inserted into pET-28a	This study
pET-*pnpE*	EcoRI-XhoI fragment containing *pnpE* inserted into pET-28a	This study
pET-*pnpF*	NdeI-XhoI fragment containing *pnpF* inserted into pET-28a	This study
pEX18Tc-*pnpA*	*pnpA* gene knockout vector containing two DNA fragments homologous to upstream and downstream regions of *pnpA* and kanamycin resistance gene	This study
pEX18Tc-*pnpA1*	*pnpA1* gene knockout vector containing two DNA fragments homologous to upstream and downstream regions of *pnpA1* and kanamycin resistance gene	This study
pRK415-*pnpA*	Vector for *pnpA* gene complementation made by fusion of *pnpA* into pRK415 at KpnI/EcoRI restriction sites	This study

min. Each sample was then centrifuged at 15,000 × *g* at 4°C for 10 min before the supernatant was collected for high-performance liquid chromatography (HPLC) analysis. For gas chromatography-mass spectrometry (GC-MS) analysis, the supernatant was extracted with ether after acidification and the extract was dried over sodium sulfate. Quantitative HPLC analysis was done by using a standard curve prepared with authentic standards. One unit of activity was defined as the amount of cells (milligrams of cell dry weight) required to transform 1 μmol of substrate per min at 30°C.

Analytical methods. HPLC was performed with a Dionex UltiMate 3000 RS HPLC system with a diode array detector (DAD) and an Agilent ZORBAX Eclipse XDB-C_{18} column (250 by 4.6 mm, 5-μm particle size). The mobile phase consisted of solvents A (0.1% acetic acid in water) and B (methanol) with a gradient program started with 30% of B, followed by an increase to 80% B from 0 to 10 min, holding at 80% B from 10 to 15 min, and then back to 30% B in 0.1 min and equilibration for 2.9 min. The flow rate was 1.0 ml/min. The column temperature was 30°C. The injection volume was 20 μl, and the wavelength range used to monitor UV absorption with the DAD was 220 to 400 nm. Under these conditions, authentic PNP, 2C4NP, 1.4-benzoquinone (BQ), CBQ, HQ, and CHQ had retention times of 8.5, 11.1, 4.5, 6.8, 3.4, and 5.2 min, respectively. The conditions used for GC-MS analysis were the same as those described previously (6), except that the mass spectrometer recorded in the range of *m*/*z* 50 to *m*/*z* 200. Under these conditions, authentic CBQ and CHQ had GC retention times of 7.6 and 11.2 min, respectively. The intermediates were identified with an NIST98 MS data library, based on comparisons of the GC retention times and mass spectra with those of authentic compounds.

Cloning of PNP and 2C4NP degradation genes and sequence analyses. To amplify a potential BQ reductase gene from strain SJ98, primers (Table 2) were designed on the basis of a conserved region of BQ reductases (accession no. C1I202 and ACZ51379) and the codon preferences of *Burkholderia* spp. The flanking regions of the fragment obtained were cloned by the genome walking strategy (18). The nucleotide sequence was determined by Tsingke BioTech Co. (Beijing, China). Analyses of open reading frames (ORFs) and amino acid identities were performed with ORF finder programs and BLASTX at the NCBI website (19).

RT-PCR and real-time PCR. Total RNA was isolated from strain SJ98 with an RNAprep pure kit for bacteria (Tiangen Biotech, Beijing, China) and reverse transcribed into cDNA with a PrimeScript RT Reagent kit (TaKaRa, Dalian, China). Reverse transcription (RT)-PCR was carried out with the primers described in Table 2. Real-time quantitative PCR (qPCR) was performed with a CFX Connect real-time PCR detection system (Bio-Rad, Hercules, CA) with iQ SYBR green Supermix (Bio-Rad, Hercules, CA) and the primers described in Table 2. A 142-bp fragment of the 16S rRNA gene of strain SJ98 was used as the reference to evaluate the relative difference in integrity between individual RNA samples. The $2^{-\Delta\Delta C_T}$ method was used to calculate relative changes in gene expression (20).

Protein expression and purification. *pnpA*, *pnpA1*, *pnpB*, *pnpCD*, *pnpE*, and *pnpF* were amplified from genomic DNA of strain SJ98 by PCR with the primers in Table 2 and cloned into pET-28a to obtain the expres-

TABLE 2 Primers used in this study

Primer	Sequence (5′–3′)[a]	Purpose
pnpA-F	GACTGACATATGGAAACGCTTGAAGGAG	Amplification of *pnpA* gene for expression
pnpA-R	GGTCTCGAGTTACGCTGCAAGCTTAAGAGG	
pnpA1-F	AGGAGACATATGATGGAGACGCTAGAAGG	Amplification of *pnpA1* gene for expression
pnpA1-R	GGCCTCGAGTCACTTCAGGACGACTTGCG	
pnpB-F	AGAAACCATATGGCAACTAAGATTCAGATTGTG	Amplification of *pnpB* gene for expression
pnpB-R	GGTCTCGAGTTACTTGGACTGCGCGACCAGC	
pnpCD-F	AGGCACCATATGCAAGAAACGGTGTTCG	Amplification of *pnpCD* gene for expression
pnpCD-R	GGACTCGAGGAACTGGATCGGATTGGC	
pnpE-F	AGGCACCATATGCAAACCCAACTCTTCATTG	Amplification of *pnpE* gene for expression
pnpE-R	GGAGAATTCTCAGCGGGGGAAGTACG	
pnpF-F	AGGCACCATATGGAACCTTTCGTATATCAAAGC	Amplification of *pnpF* gene for expression
pnpF-R	GGACTCGAGCTACCTCGGTGCCCGCC	
RTA-F	GAAGGAGTGGTCGTTGTTGGTGGAG	Amplification of 725 bp of *pnpA* by RT-PCR
RTA-R	TCGGGCATACGACGACGCACTTC	
RTB-F	AACTCGTGCCCGAAGAAGTCCTG	Amplification of 445 bp of *pnpB* by RT-PCR
RTB-R	CGAGCGATTGCCAGTTCGTTTTC	
RTA1-F	GCCTATGTGACGATTGAAACCCG	Amplification of 555 bp of *pnpA1* by RT-PCR
RTA1-R	TGCCGACTCTTTGATGACTGCG	
RTAB-F	TGCTTACACACGCAGGCACGGAC	Amplification of 743 bp of *pnpA*-*pnpB*-spanning region
RTAB-R	CGATAGCCCTTCATTCCGCTCTTAACC	
RTBA1-F	TGGTCATCGTTGGTGTGCCGTATT	Amplification of 665 bp of *pnpB*-*pnpA1*-spanning region
RTBA1-R	TCCGCCAACTACGACCACGCCTT	
RTA1C-F	CGGAAAACATTCAGAGCAGAG	Amplification of 440 bp of *pnpA1*-*pnpC*-spanning region
RTA1C-R	CCTTGCCTGTGATGATTTCG	
RTCD-F	CCGAAGGGAAAGCCGATG	Amplification of 421 bp of *pnpC*-*pnpD*-spanning region
RTCD-R	ACCGTAAAAGAAGCCCCAAGC	
RTDE-F	ACCAAATCATCTGGGACATCGC	Amplification of 459 bp of *pnpD*-*pnpE*-spanning region
RTDE-R	ACGGCACGGTCGATGTCG	
RTEF-F	AGCCCTGGTTCGCCTTTTG	Amplification of 514 bp of *pnpE*-*pnpF*-spanning region
RTEF-R	GGTCGGGATCGCAATGATAG	
RTFG-F	ATGGTCCGCAGGCTGTTTTC	Amplification of 679 bp of *pnpF*-*pnpG*-spanning region
RTFG-R	ACTTCTTCCCAGTTGCGGTCAG	
RTq16S-F	CGTGTAGCAGTGAAATGCGTAGAG	Amplification of 142-bp fragment of 16S rRNA genes for real-time qPCR
RTq16S-R	GACATCGTTTAGGGCGTGGAC	
RTq-*pnpA*-F	CGTCGCAACGAATGTCTTCTATG	Amplification of 172-bp fragment of *pnpA* for real-time qPCR
RTq-*pnpA*-R	CATACGACGACGCACTTCCTC	
RTq-*pnpA1*-F	CTGCCTATGTGACGATTGAAACC	Amplification of 134-bp fragment of *pnpA1* for real-time qPCR
RTq-*pnpA1*-R	CCAGGTGGTGCCATCAAAAG	
W-*pnpB*-F	TACAAGATGGCCGAAGC	Amplification of fragment of *pnpB* for genomic walking
W-*pnpB*-R	AGGAAGTTGCGCATTTG	
GC-*pnpA*-F	GACGGTACCGATGGAAACGCTTGAAGGAGTGG	Amplification of *pnpA* for gene complementation
GC-*pnpA*-R	GGTGAATTCTTACGCTGCAAGCTTAAGAGGC	

(Continued on following page)

TABLE 2 (Continued)

Primer	Sequence (5′–3′)[a]	Purpose
KO-pnpA$_u$-F	CCATGATTACGAATTGAGGGTTTCTAATCGGTTTCGC	Amplification of upstream fragment of *pnpA* for gene knockout
KO-pnpA$_u$-R	AGAGATTTTGAGACATTTTCAGTCTCCTGTCACAACGC	
KO-pnpA$_d$-F	GATGAGTTTTTCTAAATTTTGACCGCAATTTGGGAC	Amplification of downstream fragment of *pnpA* for gene knockout
KO-pnpA$_d$-R	GGCCAGTGCCAAGCTTTGACGCGAACCATCTGCAC	
KO-pnpA1$_u$-F	CCATGATTACGAATTGATGGCCGAAGCTATCGCG	Amplification of upstream fragment of *pnpA1* for gene knockout
KO-pnpA1$_u$-R	AGAGATTTTGAGACAGTGTCTCCTTTCAACTCGCGTTTC	
KO-pnpA1$_d$-F	GATGAGTTTTTCTAAGCGTTTGCCTTCGGAACG	Amplification of downstream fragment of *pnpA1* for gene knockout
KO-pnpA1$_d$-R	GGCCAGTGCCAAGCTTGGTGCGTCCGAATTTGTCC	
KO-kan-F	TGTCTCAAAATCTCTGATGTTAC	Amplification of kanamycin resistance gene for gene knockout
KO-kan-R	TTAGAAAAACTCATCGAGCATC	

[a] Specified restriction sites are underlined.

sion constructs listed in Table 1. The resultant plasmids were transformed into *E. coli* Rosetta(DE3)pLysS for protein expression and purification as described previously (21).

Enzyme assays. The activities of the 2C4NP and PNP 4-monooxygenase (PnpA) and CBQ and BQ reductase (PnpB) enzymes were assayed as previously described for PNP 4-monooxygenase and BQ reductase, respectively (6). The molar extinction coefficients for NAD(P)H, PNP, and 2C4NP were 6,220 M^{-1} cm^{-1} at 340 nm (22), 7,000 M^{-1} cm^{-1} at 420 nm (23), and 14,580 M^{-1} cm^{-1} at 405 nm (24), respectively. The products of H_6-PnpA- or H_6-PnpB-catalyzed reactions were identified by HPLC and GC-MS as described previously (6). The Michaelis-Menten kinetics of 2C4NP monooxygenation catalyzed by PnpA were determined by plotting reaction rates against seven concentrations of PNP (5 to 150 μM) or 2C4NP (2 to 50 μM) from three independent sets of experiments when the NADPH concentration was fixed at 400 μM. Data were fitted with the Michaelis-Menten equation by OriginPro 8 software (OriginLab, Northampton, MA). Protein concentrations were determined by the Bradford method (25) with bovine serum albumin as the standard. One unit of enzyme activity was defined as the amount of enzyme required to catalyze the disappearance of 1 μmol of substrate per min at 30°C. Specific activities are expressed in units per milligram of protein.

Detection of the enzymes involved in the sequential conversions of CHQ and HQ were performed as follows. The ring cleavage activity of CHQ and HQ dioxygenase (PnpCD) was determined by monitoring the spectral changes from 290 to 320 nm (26). For PnpCD inhibition, the reaction mixtures were incubated for 10 min with 1 mM 2,2′-dipyridyl before the addition of the substrates. The products of PnpCD-catalyzed reactions were used to detect (chloro-)4-hydroxymuconic semialdehyde dehydrogenase (PnpE) activity, which was performed by monitoring the decrease in absorption at 320 nm (3), and the increase in NADH was monitored by measuring absorption at 340 nm. In the (chloro)maleylacetate reductase (PnpF) assay, the decrease in absorption at 340 nm was used to monitor the conversion of NADH to NAD^+ as an indication of its activity (27).

Gene knockout and complementation. pEX18Tc-*pnpA* and pEX18Tc-*pnpA1* for gene knockout were constructed by fusing the upstream and downstream fragments of the target gene (*pnpA* or *pnpA1*) and the kanamycin resistance gene amplified from plasposon pTn*Mod*-Okm (28) to EcoRI/HindIII-digested pEX18Tc (29) with the In-Fusion HD Cloning kit (TaKaRa, Dalian, China) (the primers used are described in Table 2). The plasmids were then transformed into *E. coli* WM3064 before conjugation with strain SJ98 as described previously (30, 31). The SJ98Δ*pnpA* and SJ98Δ*pnpA1* double-crossover recombinants were screened on LB plates containing 10% (wt/vol) sucrose and 50 μg/ml kanamycin. pRK415-*pnpA* for gene complementation was constructed by cloning PCR products of *pnpA* into KpnI/EcoRI-digested pRK415 (32). It was transformed into *E. coli* WM3064 and then mated with *pnpA* deletion-containing strain SJ98 by conjugation to obtain SJ98Δ*pnpA*(pRK415-*pnpA*). Strain SJ98 and its derivatives were grown on 0.3 mM substrate (2C4NP or PNP), and their ability to utilize the substrate was determined by monitoring the growth of cells together with the consumption of the substrate. The growth curves were fitted by the modified Gompertz equation (33) with OriginPro 8 software, and their maximum specific growth rates (μ_m, per hour) were calculated.

RESULTS

CBQ and CHQ are metabolites of 2C4NP degradation. Strain SJ98 is able to utilize 2C4NP and PNP as a sole source of carbon and energy; however, no intermediate was initially detected by HPLC during the degradation of these two compounds. Therefore, 2,2′-dipyridyl, an iron(II) chelator used to inhibit a number of heme-dependent aromatic ring dioxygenases (26, 34), was added to the biotransformation mixtures in order to capture the intermediates. For 2C4NP degradation, two metabolites with HPLC retention times of 5.2 and 6.8 min, respectively, were accumulated with 2C4NP consumption (see Fig. S1 in the supplemental material). These two retention times precisely matched those obtained with standard CHQ and CBQ. Furthermore, the identification of CBQ and CHQ was also confirmed by GC-MS by comparison with the GC retention times and mass spectra of the authentic compounds (Fig. 1). In a biotransformation time course, 2C4NP consumption (230 μM) was approximately equivalent to the total accumulation of both CHQ (201 μM) and CBQ (12 μM) (Fig. 2), indicating nearly stoichiometric formation of CBQ and CHQ from 2C4NP. Similarly, BQ (with an HPLC retention time of 4.5 min) and HQ (retention time of 3.4 min) were detected during PNP degradation and more than 90% of the PNP (244 μM) was converted to BQ (8 μM) and HQ (217 μM) (see Fig. S2 in the supplemental material). Therefore, the identification of intermediates clearly demonstrated that strain SJ98 degraded 2C4NP with CBQ and CHQ as the intermediates before ring cleavage and degraded PNP via the typical HQ pathway (Fig. 3A).

2C4NP degradation is induced by either 2C4NP or PNP. The initial steps of 2C4NP degradation are analogous to those of PNP degradation by strain SJ98. Therefore, whole-cell biotransformation was carried out in order to investigate whether the catabolism of 2C4NP and that of PNP share the same enzymes in this strain. Negligible activity for these two nitrophenols was observed in un-

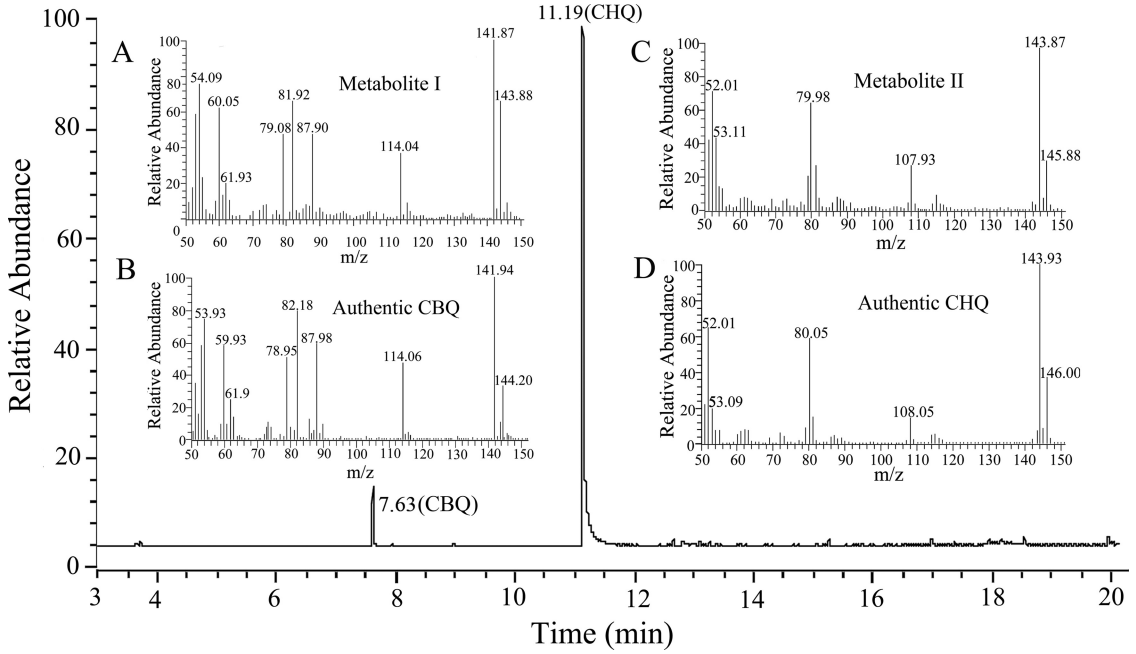

FIG 1 GC-MS analysis of the intermediates captured during 2C4NP degradation by *Burkholderia* sp. strain SJ98. Shown is the ion current chromatogram at *m*/*z* 142.00 ± 0.50 and 144.00 ± 0.50 extracted from the total ion current chromatogram. The mass spectra of metabolite I (A), authentic CBQ (B), metabolite II (C), and authentic CHQ (D) are shown within the gas chromatogram.

induced cells of strain SJ98. However, 2C4NP-induced cells exhibited a specific activity of 2.16 ± 0.52 U mg^{-1} for 2C4NP, and PNP-induced cells exhibited a specific activity of 4.86 ± 0.97 U mg^{-1} for PNP. These findings indicate that the genes encoding the enzymes involved in the catabolism of PNP and 2C4NP by strain SJ98 are inducible. Moreover, PNP-induced cells degrade 2C4NP (2.28 ± 0.18 U mg^{-1}) while strain SJ98 cells induced by 2C4NP also have the ability to degrade PNP (4.37 ± 0.34 U mg^{-1}). This indicates that the enzymes responsible for PNP catabolism are also likely to be involved in 2C4NP degradation. Interestingly, *Pseudomonas* sp. strain WBC-3, a PNP rather than 2C4NP utilizer, was also found to be able to degrade 2C4NP after PNP induction (see Fig. S3 in the supplemental material) in an experiment following the above observations in stain SJ98.

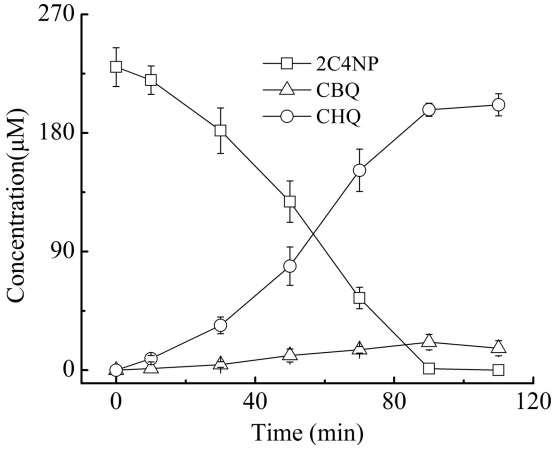

FIG 2 Time course of 2C4NP degradation by *Burkholderia* sp. strain SJ98 in whole-cell biotransformation. In order to capture the intermediates before ring cleavage, 1 mM 2,2′-dipyridyl was added to inhibit the ring cleavage enzyme. Samples were withdrawn at the time points indicated and treated immediately as described in the text. The disappearance of 2C4NP and the appearance of the products (CBQ and CHQ) were quantified by HPLC. The experiments were performed in triplicate, the results shown are average values of three independent experiments, and error bars indicate standard deviations.

Cloning and sequence analyses of the 2C4NP catabolic gene cluster. A pair of primers based on a conserved region of the BQ reductase genes was used to amplify a PCR product with an anticipated size of 242 bp from strain SJ98. Subsequently, a 17,429-bp DNA fragment extending from this 242-bp region was obtained by genome walking as outlined and annotated in the legend to Fig. 3B. The genes in this fragment have been designated the *pnp* genes, and the nucleotide sequence of this fragment is identical to that in a subsequently available draft genomic sequence of strain SJ98 (35), equivalent to nucleotides 1036909 to 1054337 of contig 12 (GenBank accession no. AJHK02000012). Among the products encoded by these genes, PnpA was reported to catalyze the monooxygenation of PNP to BQ, which was then reduced by PnpB (36), during the preparation of this report. While PnpA1 (80% identical to PnpA), PnpC, PnpD, PnpE, and PnpF exhibit high degrees of identity with the enzymes involved in PNP degradation from several PNP utilizers (3–6), PnpG has a high level of identity with the BT 1,2-dioxygenase of *Pseudomonas* sp. strain WBC-3 (37).

***pnp* genes are in a single operon that is upregulated in 2C4NP-induced cells of strain SJ98.** RT-PCR was performed with RNA derived from glucose-grown cultures of strain SJ98, with or without the addition of substrates. This showed that transcription of the *pnp* cluster was detected only under inducing conditions, and *pnpABA1CDEFG* was suggested to be in a single transcriptional operon, as shown in Fig. 3C. In addition, real-time qPCR analysis showed a 34-fold increase in gene transcription of the *pnp* cluster from the 2C4NP-induced samples, in comparison with the data from the noninduced samples. It also showed a 44-fold in-

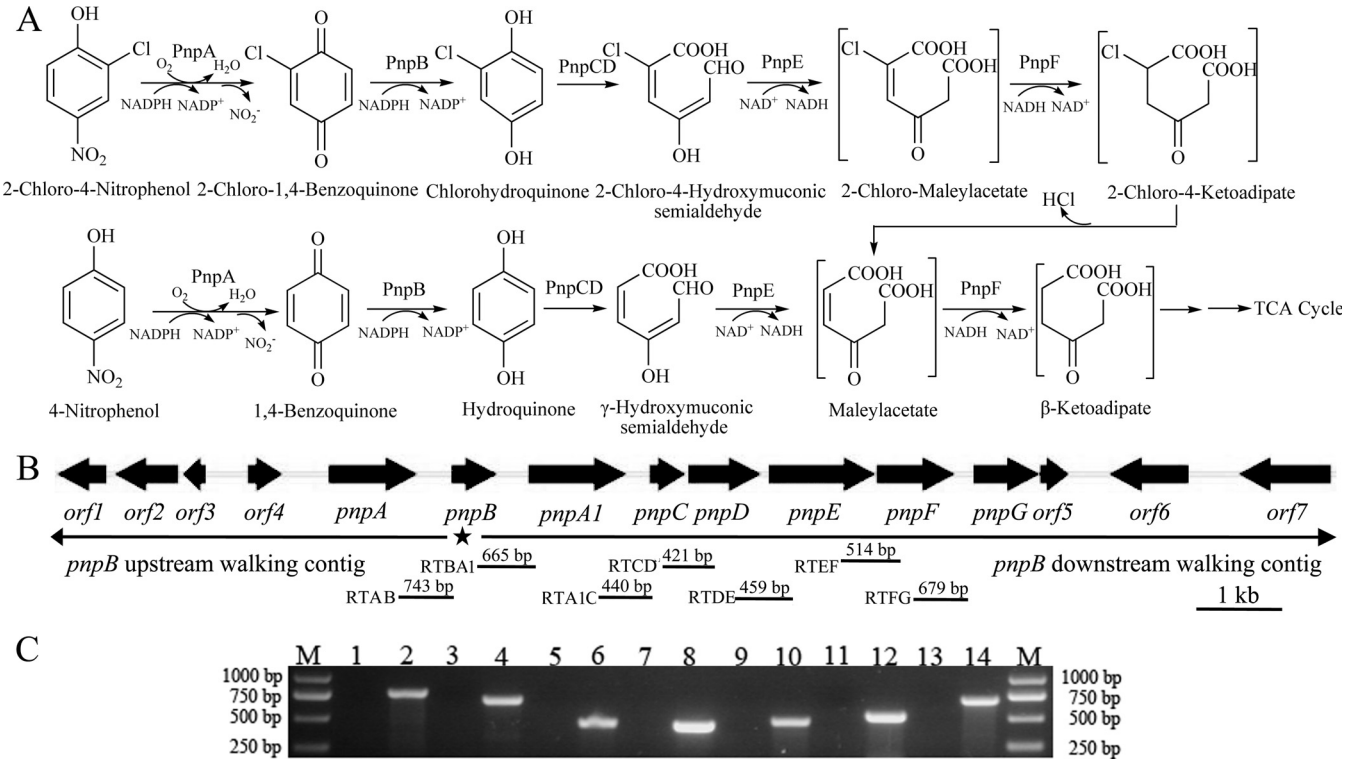

FIG 3 (A) Proposed pathways of 2C4NP and PNP catabolism in *Burkholderia* sp. strain SJ98, together with the catabolic reactions catalyzed by *pnp* gene products. The reactions catalyzed by PnpA and PnpB in PNP catabolism were suggested previously (36). TCA, tricarboxylic acid. (B) Organization of the *pnp* gene cluster of strain SJ98. The large black arrows indicate the sizes and directions of transcription of the genes and ORFs. The star below *pnpB* indicates the region where genome walking in both directions started. The locations of primer sets RTAB, RTBA1, RTA1C, RTCD, RTDE, RTEF, and RTFG and the DNA fragments amplified for RT-PCR are indicated below. (C) Analysis of *pnpABA1CDEFG* transcription by RT-PCR. Total RNAs of strain SJ98 with or without induction by 2C4NP were prepared for RT-PCR, and reactions performed without RT were used as negative controls. Lanes: M, molecular size markers; 2, 4, 6, 8, 10, 12, and 14 (template from glucose-grown strain SJ98 induced by 2C4NP), products amplified with the RTAB, RTBA1, RTA1C, RTCD, RTDE, RTEF, and RTFG primer sets, respectively, with products of RT; 1, 3, 5, 7, 9, 11, and 13, corresponding negative controls. Transcription with the template from glucose-grown strain SJ98 is not shown.

crease in gene transcription of the *pnp* cluster from PNP-induced samples.

***pnpA* is essential for strain SJ98 to utilize 2C4NP.** To investigate the physiological roles of *pnpA* and *pnpA1* in 2C4NP degradation *in vivo*, derivatives of strain SJ98 with deletion of *pnpA* or *pnpA1* were individually constructed. Strain SJ98Δ*pnpA* (with *pnpA* deleted) completely lost its ability to grow on 2C4NP, as well as PNP, and *pnpA*-complemented mutant SJ98Δ*pnpA*(pRK415-*pnpA*) regained its ability to grow on these two substrates (Fig. 4). On the other hand, in addition to a lower rate of 2C4NP or PNP removal, strain SJ98Δ*pnpA1* (with *pnpA1* deleted) also exhibited a lower growth rate than the wild type on these two substrates (Fig. 4), with its maximum specific growth rates (μ_m, per hour) being approximately 25% lower than those of wild-type SJ98 (see Table S1 in the supplemental material). In biotransformation assays, SJ98Δ*pnpA1* exhibited specific activities for 2C4NP (1.73 ± 0.45 U mg^{-1}) and PNP (3.74 ± 0.56 U mg^{-1}) approximately 20% lower than those of wild-type SJ98.

Expression and purification of enzymes involved in 2C4NP degradation. Recombinant PnpA, PnpA1, PnpB, PnpCD, PnpE, and PnpF were individually overexpressed in *E. coli* Rosetta(DE3)pLysS as N-terminally His_6-tagged fusion proteins for easy purification. H_6-PnpB, H_6-PnpCD, H_6-PnpE, and H_6-PnpF were largely soluble and readily purified, whereas only

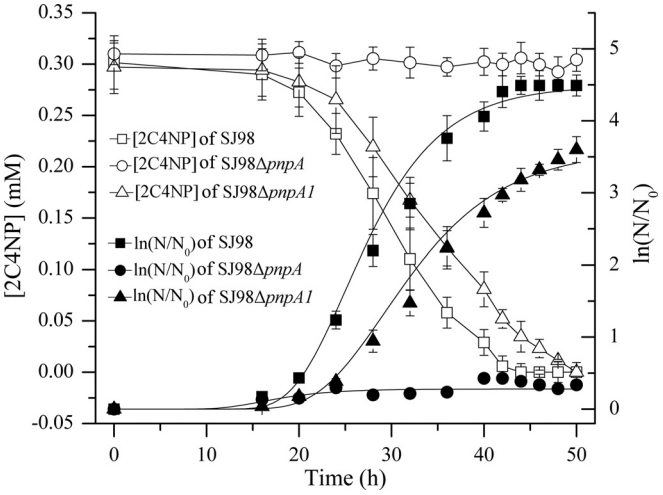

FIG 4 Time course of 2C4NP degradation and cell growth in cultures of *Burkholderia* sp. strains SJ98, SJ98Δ*pnpA* (with *pnpA* deleted), and SJ98Δ*pnpA1* (with *pnpA1* deleted). The data for *pnpA*-complemented mutant SJ98Δ*pnpA*(pRK415-*pnpA*) are not shown. The results obtained with PNP were similar to those obtained with 2C4NP (data not shown). N, number of cells; N_0, initial number of cells. The growth curves were fitted by the modified Gompertz equation (33) with OriginPro (version 8) software. All of the experiments were performed in triplicate, the results shown are average values of three independent experiments, and error bars indicate standard deviations.

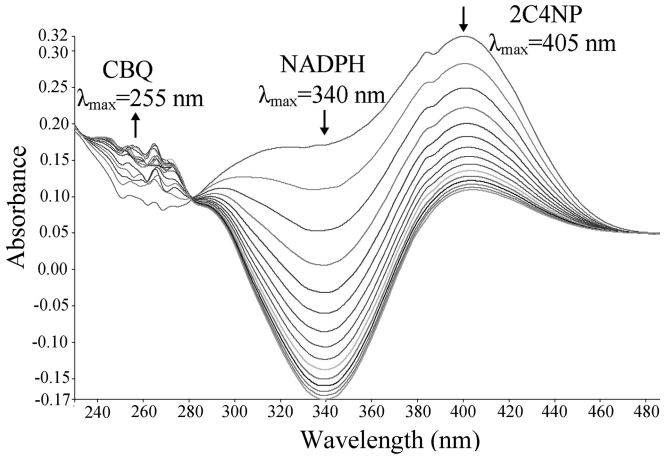

FIG 5 Spectral changes during the transformation of 2C4NP by purified H_6-PnpA. Sample and reference cuvettes contained 0.1 mM NADPH, 0.03 mM flavin adenine dinucleotide, 50 mM phosphate buffer (pH 7.4), and 10 μg H_6-PnpA in a 0.5-ml volume. The reaction was initiated by the addition of 25 μM 2C4NP, and the spectra were recorded every minute after the addition of 2C4NP. The arrows indicate the directions of spectral changes.

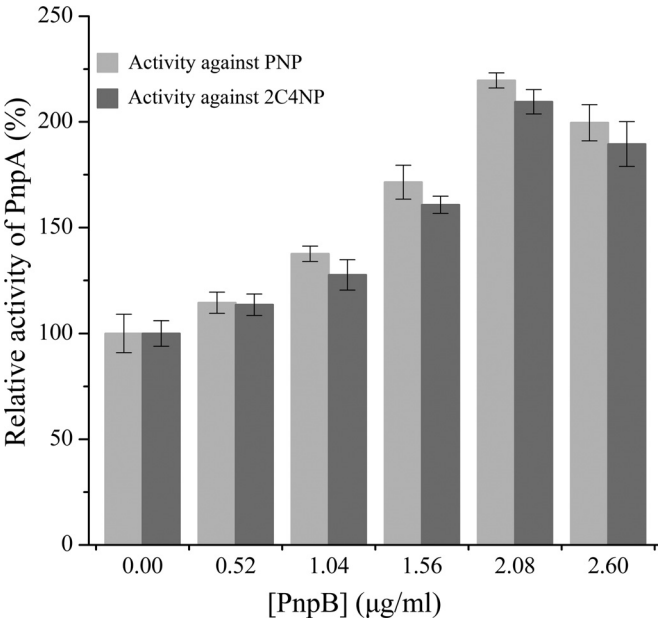

FIG 6 H_6-PnpB enhances 2C4NP and PNP degradation by H_6-PnpA. The PnpA specific activity of 7.2 U mg^{-1} against 2C4NP and 5.6 U mg^{-1} against PNP were defined as 100% when no H_6-PnpB was added.

small amounts of H_6-PnpA and H_6-PnpA1 were soluble even when *E. coli* cells were induced with 0.1 mM isopropyl-β-D-thiogalactopyranoside (IPTG) at 16°C. Therefore, the small amounts of H_6-PnpA and H_6-PnpA1 that were obtained from large quantities of cells were concentrated by ultrafiltration through an Ultra-15 filter unit with a molecular mass cutoff of 10 kDa.

In this way, a total of 0.78 mg of H_6-PnpA with a specific activity of 7.2 U mg^{-1} for 2C4NP (5.6 U mg^{-1} for PNP) was purified from 6,000 ml of culture. Even less H_6-PnpA1 was purified from 6,000 ml of culture, which hampered its further analysis *in vitro*. For H_6-PnpB purification, 28.2 mg of H_6-PnpB with a specific activity of 23.8 U mg^{-1} for CBQ (31.4 U mg^{-1} for BQ) was obtained from 1,000 ml of culture. On the other hand, 21.4 mg of H_6-PnpCD, 7.9 mg of H_6-PnpE, and 8.7 mg of H_6-PnpF were each purified from 1,000 ml of culture. SDS-PAGE analysis of all of the above purified proteins showed that the molecular masses of H_6-PnpA, H_6-PnpB, H_6-PnpC, PnpD, H_6-PnpE, and H_6-PnpF are about 45, 25, 20, 38, 55, and 40 kDa (see Fig. S4 in the supplemental material), respectively, corresponding to the molecular masses deduced from their amino acid sequences.

PnpA catalyzes the monooxygenation of 2C4NP to CBQ. In parallel to our study, it was recently reported that PnpA catalyzed the NADPH-dependent monooxygenation of PNP to BQ in PNP catabolism in this strain (36), but its role in 2C4NP degradation was not characterized. In our investigation, after the confirmation of PnpA as a PNP monooxygenase, the activity of PnpA against 2C4NP was assayed by measuring the consumption of both 2C4NP and NADPH. Rapid degradation of 2C4NP (λ_{max}, 405 nm) by H_6-PnpA occurred, as shown in Fig. 5, together with consumption of NADPH (λ_{max}, 340 nm). An isobestic point at 280 nm was observed, indicating the transformation of 2C4NP to a new product with maximum absorption at around 255 nm. By HPLC and GC-MS analyses, both CBQ (λ_{max}, 255 nm) and CHQ (λ_{max}, 291 nm) were identified as products of 2C4NP monooxygenation in the system containing purified H_6-PnpA. The detection of CHQ may be due to the nonenzymatic reduction of CBQ in the presence of NADPH, and a similar explanation was proposed previously for the production of HQ when PNP was catalyzed by PNP monooxygenases in *Pseudomonas* sp. strain WBC-3 (6) and *Arthrobacter* sp. strain JS443 (38).

Kinetic assays revealed that the K_m value of H_6-PnpA for 2C4NP (6.2 ± 0.76 μM) was lower than the value previously reported (35.4 ± 5.95 μM) (36) or that determined in this study (25.4 ± 3.63 μM) for PNP. Ironically, the PNP 4-monooxygenase (PnpA) from the PNP utilizer *Pseudomonas* sp. strain WBC-3 was also found in this study to exhibit a higher affinity and catalytic efficiency for 2C4NP (K_m = 8.1 ± 1.13 μM, k_{cat}/K_m = 1.13 ± 0.080 μM^{-1} min^{-1}) than PNP (K_m = 20.3 ± 2.70 μM, k_{cat}/K_m = 0.665 ± 0.043 μM^{-1} min^{-1}), despite its inability to grow on 2C4NP observed in this study.

PnpB catalyzes the reduction of CBQ to CHQ. Recently, PnpB was reported to catalyze the reduction of BQ in PNP catabolism (36), but its product was not identified. During this study, in addition to the HPLC identification of HQ as the product of BQ catalysis by PnpB, the activity of PnpB against CBQ was performed in order to prove the formation of CBQ during 2C4NP catabolism by strain SJ98. The product of the reaction catalyzed by H_6-PnpB was identified as CHQ by HPLC analysis. Moreover, when H_6-PnpB was added to the reaction mixture containing H_6-PnpA with 2C4NP or PNP, the activity of H_6-PnpA was enhanced significantly (Fig. 6). This is similar to the phenomenon described by Zhang et al. (6) during PNP monooxygenation in the presence of BQ reductase from strain WBC-3. A probable explanation for this enhanced activity is that the formed quinone (CBQ or BQ) is reduced by H_6-PnpB, possibly avoiding product inhibition of PnpA. In particular, the enhanced 2C4NP monooxygenase activity with H_6-PnpB in this study further demonstrates the involvement of CBQ during 2C4NP degradation by strain SJ98, apart from the GC-MS identification of CBQ as an intermediate.

Enzymatic assays of PnpCD, PnpE, and PnpF by sequential catalyses. *E. coli* cells carrying pET-*pnpCD* were found, by HPLC

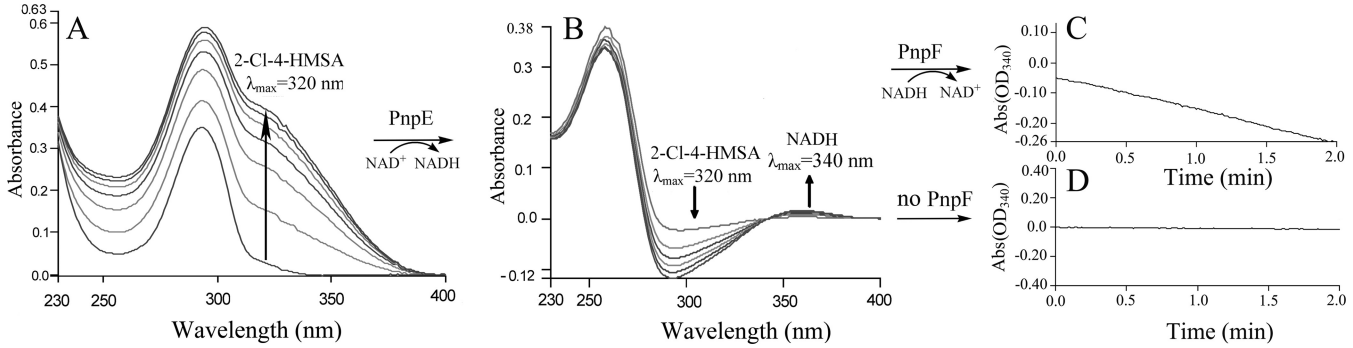

FIG 7 Assays of PnpCD, PnpE, and PnpF enzyme activities by sequential catalytic reactions with CHQ as the starting substrate. (A) Spectral changes during rapid oxidation of CHQ by purified His_6-PnpCD. Sample and reference cuvettes contained 20 mM phosphate buffer (pH 7.4), 0.04 mM Fe^{2+}, and 5 μg purified His_6-PnpCD in a 0.5-ml volume. The reaction was initiated by the addition of 0.1 mM CHQ. Spectra were recorded every minute after the addition of CHQ. (B) Enzyme activity assay of PnpE. Following the complete oxidation of CHQ to 2-chloro-4-hydroxymuconic semialdehyde by PnpCD, 50 μM NAD^+ was added to the sample cuvette from the reaction in panel A and then the contents were divided between two cuvettes (sample and reference) for assay of PnpE activity. Spectra were recorded every minute after the addition of 20 μg purified H_6-PnpE. (C, D) His_6-PnpF enzyme activity assays. Following the complete conversion of 2-chloro-4-hydroxymuconic semialdehyde to 2-chloromaleylacetate, 50 μM NADH was added to the sample cuvette from the reaction in panel B and then the contents were divided between two cuvettes (sample and reference) for assay of PnpF activity. To initiate the assay, 20 μg purified H_6-PnpF (C) or buffer without H_6-PnpF (D) was added to the sample cuvette.

analysis, to degrade HQ and CHQ, while cells harboring only the vector (pET-28a) were unable to do so. When purified His_6-PnpCD was added to the reaction mixture containing CHQ, a spectral change from 290 to 320 nm occurred to form a new peak with a λ_{max} of 320 nm (Fig. 7A), in line with the spectral property of 2-chloro-4-hydroxymuconic semialdehyde (26). On the other hand, the dioxygenase activity of PnpCD was Fe^{2+} dependent and the activity was completely abolished in the presence of the ferrous ion chelator 2,2′-dipyridyl. Sequential catalytic reactions were carried out in order to investigate whether (chloro)4-hydroxymuconic semialdehyde dehydrogenase (PnpE) and (chloro)maleylacetate reductase (PnpF) are involved in 2C4NP degradation. For the PnpE assay, the substrate contained in the reaction mixture was the ring cleavage product of CHQ from the above PnpCD-catalyzed dioxygenation, presumably, 2-chloro-4-hydroxymuconic semialdehyde. As shown in Fig. 7B, the absorbance of 2-chloro-4-hydroxymuconic semialdehyde became progressively lower after the addition of purified His_6-PnpE, together with the production of NADH, presumably forming 2-chloromaleylacetate. Following the complete oxidation of 2-chloro-4-hydroxymuconic semialdehyde by PnpE, the reaction mixture was used to assay the activity of PnpF, according to the method for assaying maleylacetate reductase from *Pseudomonas* sp. strain B13 (monitoring the decrease in the cofactor NADH by measuring absorption at 340 nm) (27). A rapid oxidation of NADH was observed (Fig. 7C) upon the addition of purified His_6-PnpF to the assay mixture, an indication of the presence of active 2-chloromaleylacetate reductase. The product of this reaction is presumably maleylacetate resulting from the dechlorination of 2-chloromaleylacetate by PnpF, similar to the reports in which maleylacetate reductases were involved in the dechlorination of 2-chloromaleylacetate to form β-ketoadipate via maleylacetate (27, 39, 40). However, no oxidation of NADH was observed when His_6-PnpF was omitted from the reaction mixture (Fig. 7D). When nonchlorinated HQ was the starting substrate, PnpCD, PnpE, and PnpF worked in the same way, in which the spectral changes are similar to those shown in Fig. 7 and the products are suggested to be 4-hydroxymuconic semialdehyde (5, 26), maleylacetate, and β-ketoadipate, respectively (41).

DISCUSSION

It was generally accepted that the BT pathway is the predominant pathway of PNP degradation by Gram-positive strains, which was initiated by a two-component PNP monooxygenase (7–11), while the HQ pathway is preferentially found in Gram-negative bacteria and is initiated by a single-component PNP monooxygenase (3–6). Previously, 2C4NP degradation by strain SJ98 was reported to be initiated by reductive dechlorination with the formation of PNP, which was further degraded via a BT pathway (Fig. 8B) (13). In this study, an initial bioinformatic analysis did not identify genes encoding the potential reductive dehalogenase or two-component PNP monooxygenase in its draft genome. Subsequent biochemical and genetic analyses demonstrated that 2C4NP metabolism in strain SJ98 occurs via the CHQ pathway rather than the BT pathway, revealing the catabolic mechanism of 2C4NP degradation at the molecular and enzymatic levels in a bacterial strain.

The 2C4NP catabolic pathway reported here is different from those of all other 2C4NP utilizers in terms of the initial reactions or the ring cleavage reaction. CHQ was identified as the ring cleavage compound in strain SJ98 (Fig. 8A), but HQ was identified as the ring cleavage compound in the previously reported degradation pathway of 2C4NP in *Rhodococcus imtechensis* RKJ 300 (14) and *Burkholderia* sp. strain RKJ 800 (Fig. 8C) (12). This clearly indicates that removal of the chloro group occurs after ring cleavage in strain SJ98, whereas the chloro group was removed before ring cleavage in other two strains. Although CHQ was also identified as the ring cleavage compound during 2C4NP degradation by *Arthrobacter* sp. strain SJCon (Fig. 8D) (1), CBQ was not detected in this case. In addition, the regioselectivity of dioxygenation of the ring cleavage substrate CHQ is remarkably different between the (chloro)hydroquinone dioxygenases of strains SJ98 and SJCon (Fig. 8A and D). The ring cleavage position of CHQ dioxygenase in cell extracts of strain SJCon was proposed in line with that of the (chloro)hydroquinone dioxygenase (LinE) from *Sphingomonas paucimobilis* UT26 (42) and the 2,6-dichlorohydroquinone dioxygenase (PcpA) from *Sphingobium chlorophenolicum* ATCC 39723 (43), splitting the ring of CHQ between C-1 and C-2 with the formation of MA (λ_{max}, 243 nm) via a transient

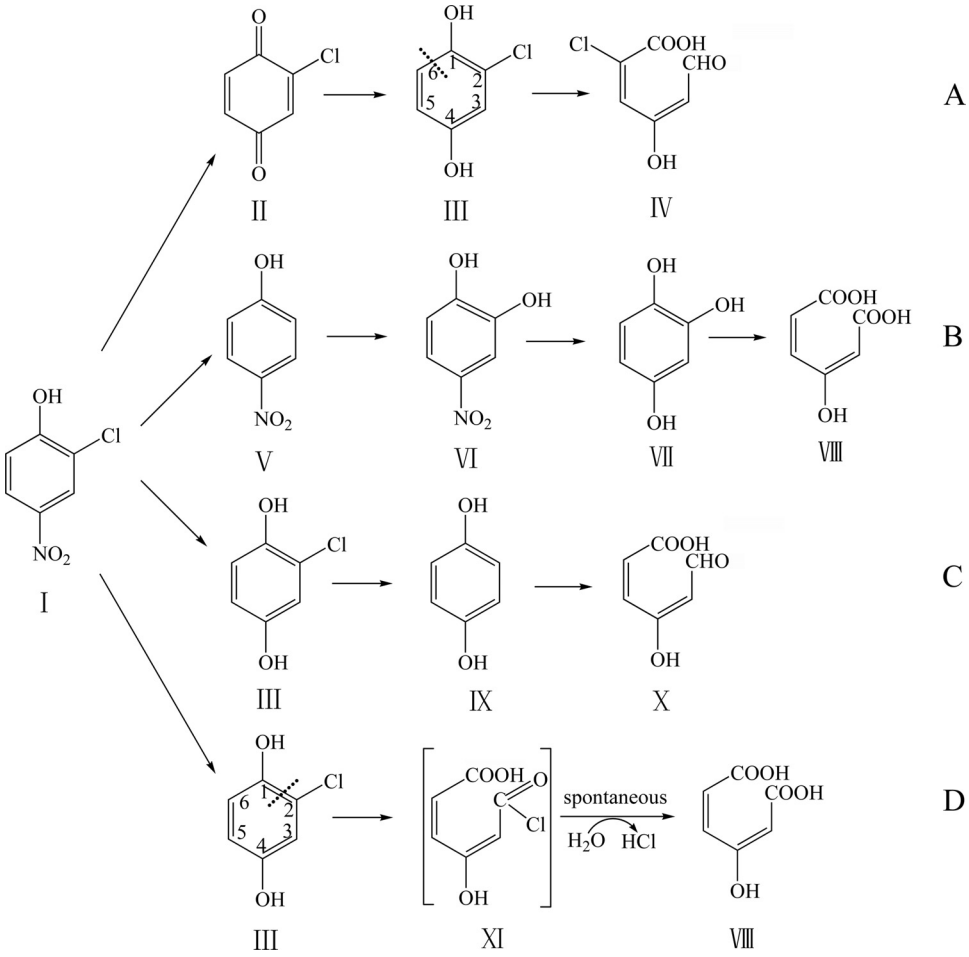

FIG 8 Proposed pathways of 2C4NP degradation by different 2C4NP utilizers. Panels: A, *Burkholderia* sp. strain SJ98 (present study); B, *Burkholderia* sp. strain SJ98 (13); C, *R. imtechensis* RKJ 300 (14) and *Burkholderia* sp. strain RKJ 800 (12); D, *Arthrobacter* sp. strain SJCon (1). The dash lines in panels A and D indicate the ring cleavage positions. Structures: I, 2C4NP; II, CBQ; III, CHQ; IV, 2-chloro-4-hydroxymuconic semialdehyde; V, PNP; VI, 4-NC; VII, BT; VIII, maleylacetate; IX, HQ; X, 4-hydroxymuconic semialdehyde; XI, acyl chloride.

intermediate (1). However, in this study, the product of CHQ catalysis by PnpCD was suggested to be 2-chloro-4-hydroxymuconic semialdehyde (λ_{max}, 320 nm), which indicated that the ring cleavage position of CHQ dioxygenase of strain SJ98 is the same as that of (chloro)hydroquinone dioxygenase (HapCD) from *Pseudomonas fluorescens* ACB (26), splitting the ring of CHQ between C-1 and C-6. Therefore, CHQ was possibly catalyzed by a LinE-like single-subunit dioxygenase in strain SJCon (although its protein sequence is unknown), whereas CHQ was split by a two-subunit dioxygenase (PnpCD) in strain SJ98.

Although three different pathways have been proposed for the microbial degradation of 2C4NP (1, 12–14), none of these pathways has been characterized at the genetic and biochemical levels. In this study, the high transcription of the *pnp* cluster in the 2C4NP-induced cell indicated that the enzymes encoded by the *pnp* cluster were likely involved in the catabolism of 2C4NP. Enzyme activity assay results and intermediate identification have shown that PnpA has the ability to catalyze the oxidation of 2C4NP to CBQ, and its encoding gene is necessary for strain SJ98 to utilize 2C4NP. The lower K_m value of PnpA for 2C4NP than PNP indicates that 2C4NP is the probable physiological substrate for PnpA in strain SJ98. In addition, the enhancement of 2C4NP monooxygenase activity of PnpA by PnpB, a reductase catalyzing the reduction of CBQ to CHQ, clearly suggests the involvement of CBQ during 2C4NP degradation. Despite the significant identity between clusters *pnpDE1E2F* and *pnpCDEF* (between 68 and 85% identity of the gene products at the amino acid level), PnpE1E2 was found to be able catalyze the ring cleavage of HQ but not CHQ (44). In contrast, PnpCD, PnpE, and PnpF, reported here, were found to be able to catalyze the sequential reactions starting from both HQ and CHQ. Considering that *pnpCDEF* are located in the same operon as *pnpAB*, it is reasonable to conclude that *pnpCDEF* are the functional genes responsible for the lower pathway of the catabolism of both 2C4NP and PNP in strain SJ98.

Unlike all other utilizers of PNP via the HQ pathway, in which the *pnp* catabolic genes are located on three operons (3–6), the genetic organization of the *pnp* cluster (*pnpABA1CDEF*) involved in the degradation of both 2C4NP and PNP in strain SJ98 is a single operon (Fig. 9), indicating its unique evolutionary pattern in acquiring 2C4NP and PNP catabolic ability. On the other hand, despite the observations that PnpA from strain WBC-3 (a well-characterized representative of the PNP utilizers) is able to catalyze the monooxygenation of both PNP and 2C4NP and all other Pnp proteins share significant homology with their counterparts

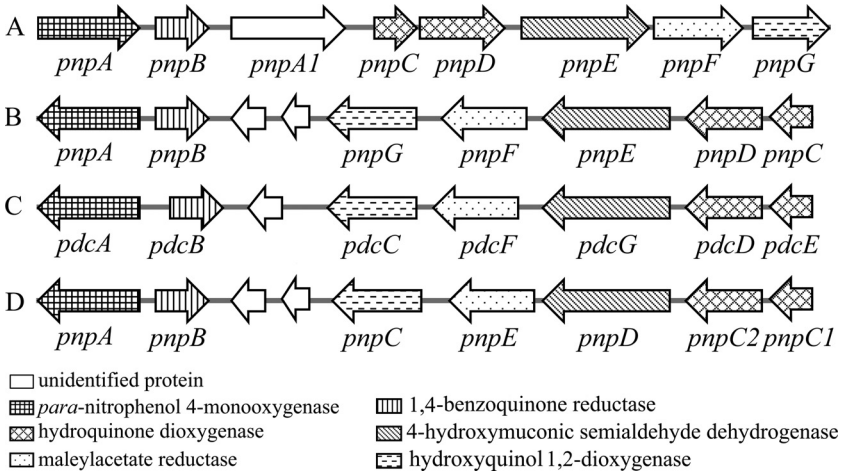

FIG 9 Comparison of the genetic organization of PNP catabolic clusters from different PNP utilizers. Panels: A, *Burkholderia* sp. strain SJ98 (accession no. AJHK02000012) (35); B, *Pseudomonas* sp. strain WBC-3 (accession no. EF577044) (6) and *Pseudomonas* sp. strain NyZ402 (accession no. GU123925) (4); C, *Pseudomonas* sp. strain 1-7 (accession no. FJ821777) (3); D, *Pseudomonas putida* DLL-E4 (accession no. FJ376608) (5).

in strain SJ98, strain WBC-3 does not grow on 2C4NP. Nevertheless, it is able to degrade 2C4NP after PNP induction. These observations suggest that different regulatory mechanisms are involved in the initiation of *pnp* gene transcription in strains SJ98 and WBC-3.

ACKNOWLEDGMENTS

This work was supported by the National Natural Science Foundation of China (grant 31270103) and the National Key Basic Research Program of China (973 Program, grant 2012CB725202).

We are grateful to the Core Facility and Technical Support in the Wuhan Institute of Virology, Chinese Academy of Sciences.

REFERENCES

1. **Arora PK, Jain RK.** 2011. Pathway for degradation of 2-chloro-4-nitrophenol in *Arthrobacter* sp. SJCon. Curr. Microbiol. **63:**568–573. http://dx.doi.org/10.1007/s00284-011-0022-2.
2. **Arora PK, Sasikala C, Ramana ChV.** 2012. Degradation of chlorinated nitroaromatic compounds. Appl. Microbiol. Biotechnol. **93:**2265–2277. http://dx.doi.org/10.1007/s00253-012-3927-1.
3. **Zhang S, Sun W, Xu L, Zheng X, Chu X, Tian J, Wu N, Fan Y.** 2012. Identification of the *para*-nitrophenol catabolic pathway, and characterization of three enzymes involved in the hydroquinone pathway, in *Pseudomonas* sp. 1-7. BMC Microbiol. **12:**27. http://dx.doi.org/10.1186/1471-2180-12-27.
4. **Wei Q, Liu H, Zhang JJ, Wang SH, Xiao Y, Zhou NY.** 2010. Characterization of a *para*-nitrophenol catabolic cluster in *Pseudomonas* sp. strain NyZ402 and construction of an engineered strain capable of simultaneously mineralizing both *para*- and *ortho*-nitrophenols. Biodegradation **21:**575–584. http://dx.doi.org/10.1007/s10532-009-9325-4.
5. **Shen W, Liu W, Zhang J, Tao J, Deng H, Cao H, Cui Z.** 2010. Cloning and characterization of a gene cluster involved in the catabolism of *p*-nitrophenol from *Pseudomonas putida* DLL-E4. Bioresour. Technol. **101:**7516–7522. http://dx.doi.org/10.1016/j.biortech.2010.04.052.
6. **Zhang JJ, Liu H, Xiao Y, Zhang XE, Zhou NY.** 2009. Identification and characterization of catabolic *para*-nitrophenol 4-monooxygenase and *para*-benzoquinone reductase from *Pseudomonas* sp. strain WBC-3. J. Bacteriol. **191:**2703–2710. http://dx.doi.org/10.1128/JB.01566-08.
7. **Yamamoto K, Nishimura M, Kato DI, Takeo M, Negoro S.** 2011. Identification and characterization of another 4-nitrophenol degradation gene cluster, *nps*, in *Rhodococcus* sp. strain PN1. J. Biosci. Bioeng. **111:**687–694. http://dx.doi.org/10.1016/j.jbiosc.2011.01.016.
8. **Liu PP, Zhang JJ, Zhou NY.** 2010. Characterization and mutagenesis of a two-component monooxygenase involved in *para*-nitrophenol degradation by an *Arthrobacter* strain. Int. Biodeter. Biodegr. **64:**293–299. http://dx.doi.org/10.1016/j.ibiod.2010.03.001.
9. **Takeo M, Murakami M, Niihara S, Yamamoto K, Nishimura M, Kato D, Negoro S.** 2008. Mechanism of 4-nitrophenol oxidation in *Rhodococcus* sp. strain PN1: characterization of the two-component 4-nitrophenol hydroxylase and regulation of its expression. J. Bacteriol. **190:**7367–7374. http://dx.doi.org/10.1128/JB.00742-08.
10. **Kitagawa W, Kimura N, Kamagata Y.** 2004. A novel *p*-nitrophenol degradation gene cluster from a Gram-positive bacterium, *Rhodococcus opacus* SAO101. J. Bacteriol. **186:**4894–4902. http://dx.doi.org/10.1128/JB.186.15.4894-4902.2004.
11. **Kadiyala V, Spain JC.** 1998. A two-component monooxygenase catalyzes both the hydroxylation of *p*-nitrophenol and the oxidative release of nitrite from 4-nitrocatechol in *Bacillus sphaericus* JS905. Appl. Environ. Microbiol. **64:**2479–2484.
12. **Arora PK, Jain RK.** 2012. Metabolism of 2-chloro-4-nitrophenol in a gram negative bacterium, *Burkholderia* sp RKJ 800. PLoS One **7**(6): e38676. http://dx.doi.org/10.1371/journal.pone.0038676.
13. **Pandey J, Heipieper HJ, Chauhan A, Arora PK, Prakash D, Takeo M, Jain RK.** 2011. Reductive dehalogenation mediated initiation of aerobic degradation of 2-chloro-4-nitrophenol (2C4NP) by *Burkholderia* sp. strain SJ98. Appl. Microbiol. Biotechnol. **92:**597–607. http://dx.doi.org/10.1007/s00253-011-3254-y.
14. **Ghosh A, Khurana M, Chauhan A, Takeo M, Chakraborti AK, Jain RK.** 2010. Degradation of 4-nitrophenol, 2-chloro-4-nitrophenol, and 2,4-dinitrophenol by *Rhodococcus imtechensis* strain RKJ300. Environ. Sci. Technol. **44:**1069–1077. http://dx.doi.org/10.1021/es9034123.
15. **Chauhan A, Pandey G, Sharma NK, Paul D, Pandey J, Jain RK.** 2010. *p*-Nitrophenol degradation via 4-nitrocatechol in *Burkholderia* sp. SJ98 and cloning of some of the lower pathway genes. Environ. Sci. Technol. **44:**3435–3441. http://dx.doi.org/10.1021/es9024172.
16. **Liu H, Wang SJ, Zhang JJ, Dai H, Tang H, Zhou NY.** 2011. Patchwork assembly of *nag*-like nitroarene dioxygenase genes and the 3-chlorocatechol degradation cluster for evolution of the 2-chloronitrobenzene catabolism pathway in *Pseudomonas stutzeri* ZWLR2-1. Appl. Environ. Microbiol. **77:**4547–4552. http://dx.doi.org/10.1128/AEM.02543-10.
17. **Chen YF, Chao H, Zhou NY.** 2014. The catabolism of 2,4-xylenol and *p*-cresol share the enzymes for the oxidation of *para*-methyl group in *Pseudomonas putida* NCIMB 9866. Appl. Microbiol. Biotechnol. **98:**1349–1356. http://dx.doi.org/10.1007/s00253-013-5001-z.
18. **Siebert PD, Chenchik A, Kellogg DE, Lukyanov KA, Lukyanov SA.** 1995. An improved PCR method for walking in uncloned genomic DNA. Nucleic Acids Res. **23:**1087–1088. http://dx.doi.org/10.1093/nar/23.6.1087.
19. **Ye J, McGinnis S, Madden TL.** 2006. BLAST: improvements for better sequence analysis. Nucleic Acids Res. **34:**W6–W9. http://dx.doi.org/10.1093/nar/gkl164.

20. **Livak KJ, Schmittgen TD.** 2001. Analysis of relative gene expression data using real-time quantitative PCR and the $2^{-\Delta\Delta C_T}$ method. Methods **25:** 402–408. http://dx.doi.org/10.1006/meth.2001.1262.
21. **Liu TT, Zhou NY.** 2012. Novel L-cysteine-dependent maleylpyruvate isomerase in the gentisate pathway of *Paenibacillus* sp. strain NyZ101. J. Bacteriol. **194:**3987–3994. http://dx.doi.org/10.1128/JB.00050-12.
22. **Fontecave M, Eliasson R, Reichard P.** 1987. NAD(P)H:flavin oxidoreductase of *Escherichia coli*. A ferric iron reductase participating in the generation of the free radical of ribonucleotide reductase. J. Biol. Chem. **262:**12325–12331.
23. **Spain JC, Wyss O, Gibson DT.** 1979. Enzymatic oxidation of *p*-nitrophenol. Biochem. Biophys. Res. Commun. **88:**634–641. http://dx.doi.org/10.1016/0006-291X(79)92095-3.
24. **Winn-Deen ES, David H, Sigler G, Chavez R.** 1988. Development of a direct assay for α-amylase. Clin. Chem. **34:**2005–2008.
25. **Bradford MM.** 1976. A rapid and sensitive method for the quantitation of microgram quantities of protein utilizing the principle of protein-dye binding. Anal. Biochem. **72:**248–254. http://dx.doi.org/10.1016/0003-2697(76)90527-3.
26. **Moonen MJ, Synowsky SA, van den Berg WA, Westphal AH, Heck AJ, van den Heuvel RH, Fraaije MW, van Berkel WJ.** 2008. Hydroquinone dioxygenase from *Pseudomonas fluorescens* ACB: a novel member of the family of nonheme-iron(II)-dependent dioxygenases. J. Bacteriol. **190:** 5199–5209. http://dx.doi.org/10.1128/JB.01945-07.
27. **Kaschabek SR, Reineke W.** 1995. Maleylacetate reductase of *Pseudomonas* sp. strain B13: specificity of substrate conversion and halide elimination. J. Bacteriol. **177:**320–325.
28. **Dennis JJ, Zylstra GJ.** 1998. Plasposons: modular self-cloning minitransposon derivatives for rapid genetic analysis of Gram-negative bacterial genomes. Appl. Environ. Microbiol. **64:**2710–2715.
29. **Hoang TT, Karkhoff-Schweizer RR, Kutchma AJ, Schweizer HP.** 1998. A broad-host-range Flp-FRT recombination system for site-specific excision of chromosomally-located DNA sequences: application for isolation of unmarked *Pseudomonas aeruginosa* mutants. Gene **212:**77–86. http://dx.doi.org/10.1016/S0378-1119(98)00130-9.
30. **Dehio C, Meyer M.** 1997. Maintenance of broad-host-range incompatibility group P and group Q plasmids and transposition of Tn*5* in *Bartonella henselae* following conjugal plasmid transfer from *Escherichia coli*. J. Bacteriol. **179:**538–540.
31. **Saltikov CW, Newman DK.** 2003. Genetic identification of a respiratory arsenate reductase. Proc. Natl. Acad. Sci. U. S. A. **100:**10983–10988. http://dx.doi.org/10.1073/pnas.1834303100.
32. **Keen NT, Tamaki S, Kobayashi D, Trollinger D.** 1988. Improved broad-host-range plasmids for DNA cloning in gram-negative bacteria. Gene **70:**191–197. http://dx.doi.org/10.1016/0378-1119(88)90117-5.
33. **Zwietering MH, Jongenburger I, Rombouts FM, Vantriet K.** 1990. Modeling of the bacterial-growth curve. Appl. Environ. Microbiol. **56:** 1875–1881.
34. **Ferreira MI, Marchesi JR, Janssen DB.** 2008. Degradation of 4-fluorophenol by *Arthrobacter* sp. strain IF1. Appl. Microbiol. Biotechnol. **78:** 709–717. http://dx.doi.org/10.1007/s00253-008-1343-3.
35. **Kumar S, Vikram S, Raghava GP.** 2012. Genome sequence of the nitroaromatic compound-degrading bacterium *Burkholderia* sp. strain SJ98. J. Bacteriol. **194:**3286. http://dx.doi.org/10.1128/JB.00497-12.
36. **Vikram S, Pandey J, Kumar S, Raghava GP.** 2013. Genes involved in degradation of *para*-nitrophenol are differentially arranged in form of non-contiguous gene clusters in *Burkholderia* sp. strain SJ98. PLoS One **8**(12):e84766. http://dx.doi.org/10.1371/journal.pone.0084766.
37. **Wei M, Zhang JJ, Liu H, Zhou NY.** 2010. *para*-Nitrophenol 4-monooxygenase and hydroxyquinol 1,2-dioxygenase catalyze sequential transformation of 4-nitrocatechol in *Pseudomonas* sp. strain WBC-3. Biodegradation **21:**915–921. http://dx.doi.org/10.1007/s10532-010-9351-2.
38. **Perry LL, Zylstra GJ.** 2007. Cloning of a gene cluster involved in the catabolism of *p*-nitrophenol by *Arthrobacter* sp. strain JS443 and characterization of the *p*-nitrophenol monooxygenase. J. Bacteriol. **189:**7563–7572. http://dx.doi.org/10.1128/JB.01849-06.
39. **Vollmer MD, Stadlerfritzsche K, Schlomann M.** 1993. Conversion of 2-chloromaleylacetate in *Alcaligenes eutrophus* JMP134. Arch. Microbiol. **159:**182–188. http://dx.doi.org/10.1007/BF00250280.
40. **Kaschabek SR, Reineke W.** 1992. Maleylacetate reductase of *Pseudomonas* sp. strain B13: dechlorination of chloromaleylacetates, metabolites in the degradation of chloroaromatic compounds. Arch. Microbiol. **158:** 412–417.
41. **Spain JC, Gibson DT.** 1991. Pathway for biodegradation of *p*-nitrophenol in a *Moraxella* sp. Appl. Environ. Microbiol. **57:**812–819.
42. **Miyauchi K, Adachi Y, Nagata Y, Takagi M.** 1999. Cloning and sequencing of a novel *meta* cleavage dioxygenase gene whose product is involved in degradation of γ-hexachlorocyclohexane in *Sphingomonas paucimobilis*. J. Bacteriol. **181:**6712–6719.
43. **Ohtsubo Y, Miyauchi K, Kanda K, Hatta T, Kiyohara H, Senda T, Nagata Y, Mitsui Y, Takagi M.** 1999. PcpA, which is involved in the degradation of pentachlorophenol in *Sphingomonas chlorophenolica* ATCC 39723, is a novel type of ring cleavage dioxygenase. FEBS Lett. **459:**395–398. http://dx.doi.org/10.1016/S0014-5793(99)01305-8.
44. **Vikram S, Pandey J, Kumar S, Raghava GP.** 2013. Genes involved in degradation of *para*-nitrophenol are differentially arranged in form of non-contiguous gene clusters in *Burkholderia* sp. strain SJ98. PLoS One **8**(12):e84766. http://dx.doi.org/10.1371/journal.pone.0084766.